IDENTIFYING ANCIENT DUNE PROCESSES IN THE STIMSON FORMATION OF GALE CRATER USING GEOCHEMICAL DATA FROM CHEMCAM: NEW INSIGHTS FROM THE GREENHEUGH CAPPING UNIT.

C. C. Bedford[1,2], S. Banham[3], D. Bowden[4], J. C. Bridges[4], R. Smith[5], O. Forni[6], A. Cousin[6], F. Rivera-Hernandez[7], C. Achilles[8], E. Dehouck[9], R. C. Wiens[10], K. Rammelkamp[6], P.Gasda[10], J. Frydenvang[11], O. Gasnault[6], E. B. Rampe[2], and S. P. Schwenzer[12], and A. A. Bryk[13] [1]Lunar and Planetary Institute, USRA, USA (cbedford@lpi.usra.edu), [2]ARES, NASA Johnson Space Center, USA, [3]Imperial College, UK, [4]University of Leicester, UK, [5]Stony Brook University, USA, [6]IRAP, Toulouse, France, [7]Georgia Tech, USA, [8]NASA Goddard, USA [9]University of Lyon, France, [10]LANL, USA, [11]University of Copenhagen, Denmark, [12]The Open University, UK, [13]University of California, Berkeley.

Introduction: The Stimson formation of Gale crater is an aeolian sandstone that unconformably overlies the fluviolacustrine units of the Murray formation [1,2]. As such, the Stimson fm. is so far the youngest in situ geological unit visited by the NASA Curiosity rover and offers a window into the environmental conditions of Gale crater's relatively recent geological history after the fluviolacustrine units were deposited but at a time when groundwater was still present to cement the sandstone. **In this study, we use geochemical data from the ChemCam instrument onboard Curiosity to constrain sandstone diagenesis, identify geochemical variations relating to net-sediment transport direction, and determine variations in sediment source in the lithified Stimson aeolian sandstone.**

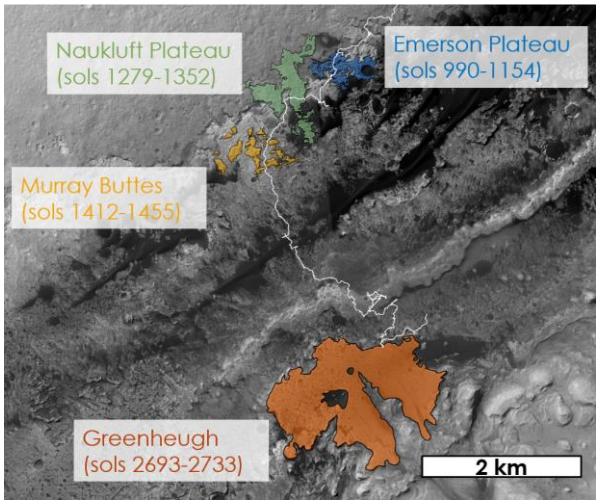

Figure 1: An annotated map showing the localities of the Stimson formation and the rover's traverse (white line).

Methods: Curiosity investigated the Stimson fm. at three localities along its traverse (Fig. 1); the Emerson Plateau (EP), Naukluft Plateau (NP), and most recently at the Greenheugh Pediment (GP). Geochemical and mineralogical data of the Stimson fm. were collected by the ChemCam, Alpha-Particle X-ray Spectrometer (APXS), and CheMin X-ray diffractometer instruments.

ChemCam uses Laser-Induced Breakdown Spectroscopy to acquire geochemical data of geological targets up to 7 m from the rover mast [3]. We have sorted and classified the ChemCam observation point analyses of the Stimson fm. according to whether an alteration feature (e.g., fracture fill), float, soil, or bedrock was targeted. The bedrock dataset was further refined to exclude all ChemCam data with totals outside a range of 90–105 wt% to further reduce the influence of hydrated phases The ChemCam data were then compared across all sites using a density analysis, equivalence tests, and a multivariate cluster analysis to distinguish geochemical trends associated with aqueous alteration and discern variations in detrital igneous mineralogy. The latter could relate to mineral sorting or changes in sediment source. Finally, we compare the ChemCam data to the mineralogical and geochemical data from the CheMin and APXS instruments, respectively.

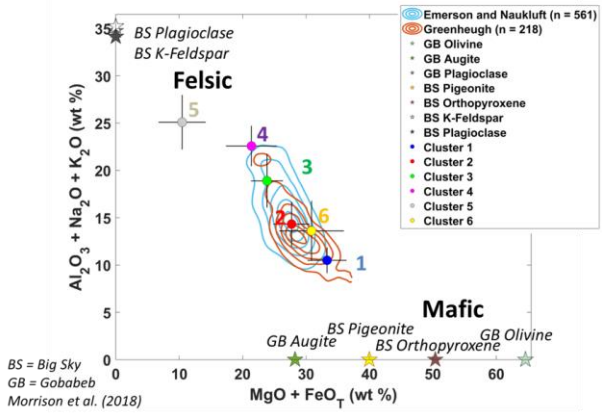

Figure 2: A bivariate plot showing the bulk geochemical compositions of EP, NP, and GP Stimson alongside the average compositions of the derived clusters and their standard deviations. Axes show Al_2O_3 + Na_2O + K_2O against MgO + FeO_T. Stars represent the mafic and felsic minerals detected in modern (GB) and lithified aeolian sediments (BS) [4].

Results: The geochemical range of the Stimson formation bedrock is similar across all localities, but the distributions and average compositions vary. EP

and NP are most similar to each other, but on average EP has higher MgO and lower Al_2O_3, Na_2O, and K_2O relative to NP. Stimson at GP has higher average MgO concentrations and lower Al_2O_3 and SiO_2 concentrations than both EP and NP (Fig. 2).

A multivariate cluster analysis of the Stimson fm. host rock dataset produces six clusters (Fig. 2). Clusters 1 (n = 53) and 2 (n = 527) have the highest FeO_T concentrations, with Cluster 1 having more MgO than Cluster 2, which in turn has more CaO. Clusters 3 (n = 156), 4 (n = 16), and 5 (n = 9) derive a cluster subset that has the most SiO_2, Al_2O_3, CaO, Na_2O and K_2O. Cluster 3 has more CaO than 4 and 5, Cluster 4 has more Na_2O and Cluster 5 has the most SiO_2, Al_2O_3 and K_2O. Finally, Cluster 6 (n = 4) is the smallest cluster and consists of ChemCam observation points with the most MnO.

Aqueous alteration: Some open-system alteration features such as fracture-associated silica-rich halos and calcium-sulfate mineral veins are present within the Stimson bedrock at EP and NP, though their occurrence is less common than in the mudstones below the unconformity [5,6]. Calcium-sulfate mineral veins are present at GP, but these are rare, and halos have not been identified yet suggesting that the alteration event that formed these features at EP and NP did not extend towards GP.

Concretions are present at all Stimson localities and likely formed isochemically as their geochemistry is equivalent to that of non-concretionary bedrock [7]. Concretions do not distort the sedimentary features in the bedrock and thereby likely formed during the lithification of the bedrock as areas of preferential cementation [2,7]. The sandstone cements of EP and NP are similar to each other and likely consist of hematite, magnetite and/or an amorphous component [6]. The sandstone cement of GP is different from EP and NP in that it likely consists of magnetite and phyllosilicates in addition to an amorphous component [8]. The difference in the secondary mineral phases between EP & NP compared to GP suggests that GP experienced different aqueous alteration and diagenesis. Although GP has phyllosilicates, it also contains abundant ~8 wt% olivine [8] which suggests that open-system alteration at this locality was limited, as also indicated by low Chemical Index of Alteration (CIA) values.

Mineral sorting or sediment source: The lack of evidence for substantial open-system alteration at all Stimson fm. locations examined to date suggests that the geochemical effects of mineral sorting regimes or changes in sediment source may have been preserved.

Cluster analysis results combined with mineral compositional data from CheMin show that these geochemical variations between the localities likely relate to differences in the relative abundance of mafic and felsic minerals (Fig. 2). EP has a slightly higher proportion of data (73%) associated with mafic clusters 1 and 2 than NP (71%). GP has the highest proportion of data associated with mafic clusters overall (89%). Results from physical abrasion experiments on basaltic sediments and terrestrial analog studies show that mafic minerals and volcanic glass are transported farther in dry aeolian environments as they have a higher physical durability [9,10]. This suggests that the dunes migrated SW-NE from NP to EP supporting the interpretation of [2]. Mineral sorting is unlikely to have concentrated mafic components to a greater degree at GP as the cross-set dip directions indicate that GP should have experienced less transport [11] and hence be more felsic than mafic. Instead, it is possible that the sediments preserved at GP may be from a more olivine-rich sediment source compared to those preserved at EP and NP.

Evidence of sediment recycling contributing to the Stimson fm. exists as mudstone rip-up clasts situated at the base of the Stimson fm. in EP [12]. EP and NP also have a similar bulk geochemical composition to that of the subalkaline basalt endmember of the Bradbury group fluviolacustrine units that were encountered early in the mission on the crater floor suggesting either a similar source or recycling of the older Bradbury materials by the Stimson dunes preserved at EP and NP [7]. As the Stimson fm. at GP is located several km away from EP and NP, it is possible that its mineralogy and geochemistry reflects the recycling of a more olivine-rich and local sediment source such as the marker beds situated just above the Greenheugh capping unit farther up the slopes of Mt. Sharp [13].

Acknowledgments: CCB was funded by the NASA PSTAR program. SPS and JCB acknowledge UKSA Aurora funding. Mission support from NASA's Mars Exploration Program is gratefully acknowledged.

References: [1] Banham S. et al. (2018) doi: 10.1111/sed.12469. [2] Watkins J. et al. (2016) *47th LPSC, Abstract #1903*. [3] Wiens R. C. et al. (2012) doi: 10.1007/s11214-012-9902-4. [4] Morrison S. et al. (2018) doi: 10.2138/am-2018-6124. [5] Frydenvang J. et al. (2017) doi: 10.1002/2017GL073323. [6] Yen A. et al. (2017) doi: 10.1016/j.epsl.2017.04.33. [7] Bedford C. C. et al. (2020) doi: 10.1016/j.icarus.2020.113622. [8] Rampe et al. (2020) AGU Fall Meeting, Abstract # P070-09. [9] Cornwall C. et al. (2015) doi: 10.1016/j.icarus.2015.04.020. [10] Mangold N. et al. (2011) doi: 10.1016/j.epsl.2011.07.025. [11] Banham S. et al. (2020) AGU. [12] Newsom H. et al. (2016) *47th LPSC Abstract #2497*. [13] Rudolph A. et al. (2019) *50th LPSC Abstract #1914.*